Asociación Argentina
de Mecánica Computacional

Mecánica Computacional Vol XLII, pp. 703-712
A. Caggiano, G. Etse, P. Folino, M. Goldschmit, M. Pucheta, M. Storti (Eds.)
P. Folino, M. Ripani, S. Vrech (Issue eds.)
Buenos Aires, November 11-14, 2025

# COMPARATIVE MODELING OF QUASI BRITTLE FRACTURE USING A TRUSS-BASED DISCRETE ELEMENT METHOD AND A PHASE FIELD FORMULATION

**Javier A. Zambrano-Carrillo[a], Ignacio Iturrioz[b], P.J. Sánchez[a,c] and Alfredo E. Huespe[a,d]**

[a]*CIMEC-UNL-CONICET, Guemes 3450, CP 3000 Santa Fe, Argentina, zambranoj88@cimec.unl.edu.ar, psanchez@cimec.unl.edu.ar, ahuespe@cimec.unl.edu.ar, https://cimec.conicet.gov.ar*

[b]*Applied Mechanical Group GMAP, Mechanical Engeneering Post Graduation Program, Federal University of Rio Grande do Sul, Rua Sarmento Leite, 425, Porto Alegre 90040-001, Brazil, ignacio.iturrioz@ufrgs.br, https://www.ufrgs.br/gmap/*

[c]*GIMNI-UTN-FRSF, Lavaise 610, CP 3000 Santa Fe, Argentina, gimni@frsf.utn.edu.ar, https://www.frsf.utn.edu.ar/*

[d]*Programa de Engenharia Mecânica - COPPE, Universidade Federal do Rio de Janeiro, Cidade Universitária, Rio de Janeiro, CEP 21941-972, RJ, Brazil, diretoria@coppe.ufrj.br, https://coppe.ufrj.br/*

**Keywords:** Quasi Brittle Materials, Fracture Mechanics, Discrete Element Method (DEM), Phase Field Method (PFM), Numerical modeling of cracks, Strength and Toughness.

**Abstract.** This work presents a comparative study between two numerical approaches for modeling fracture in quasi-brittle materials: the truss-based Discrete Element Method (DEM) and the Phase Field Method (PFM), formulated within the Finite Element Method (FEM) framework. In the version of the Discrete Element Method used here (referred to as DEM), the spatial discretization is performed using a regular arrangement of pinned bars with masses concentrated at the nodes. The equivalent cross-sectional area of the diagonal and normal bars allows the representation of an equivalent elastic solid. To capture the nonlinear mechanical behaviour produced for the evolution of the material damage, a bilinear constitutive law is applied to each bar. This formulation enables the definition of a motion equation that must be integrated in time using an explicit scheme, such as the central difference finite difference method. An important feature of the present model is its ability to incorporate material properties as random fields. In contrast, the phase field model introduces a scalar damage field to describe fracture as a continuous transition in the medium, and in this work, it is implemented based on the Principle of Virtual Work. To compare the performance of both methods, three examples are presented. A Single Edge Notch Bending (SENB) performed in epoxy resin, a Notched Plate with Hole (NPWH) also built in cement mortar, and finally a parametric study where the influence of the material parameters of a specimen composed of a substrate, and an interface orthogonal to the crack propagation direction is analyzed. The comparison of the two approaches through these three examples allows the identification of the strengths and weaknesses of each method.


ISSN: 2591-3522 DOI: 10.70567/mc.v42.ocsid8273

## 1 INTRODUCTION

Fracture in quasi-brittle materials, such as concrete, rocks, ceramics, and certain polymers, remains a central challenge in computational mechanics. The heterogeneous microstructure of these materials induces complex cracking phenomena including initiation, propagation, branching, and coalescence of cracks whose accurate description is crucial not only for ensuring structural safety but also for guiding the design of materials with enhanced toughness and damage tolerance.

Traditional numerical methods, including the Finite Element Method (FEM) and the Boundary Element Method (BEM), have been extensively applied in fracture mechanics. However, being rooted in continuum formulations, these methods face inherent limitations when simulating crack evolution. The need for remeshing, enrichment techniques, or explicit crack tracking often renders their application computationally expensive and, in some cases, numerically unstable. Strategies such as the Extended Finite Element Method (XFEM) or Cohesive Zone Models (CZM) have alleviated some of these difficulties, but they still exhibit restrictions when dealing with complex crack paths or capturing the effects of microstructural heterogeneity (Kosteski et al. (2011); Zambrano et al. (2022)).

To overcome these limitations, alternative methodologies have emerged in recent decades. Among them, the Discrete Element Method (DEM), particularly in truss-based formulations, has gained attention. In this approach, the solid is represented by a network of uniaxial elements with lumped masses at their nodes. Fracture is modeled directly through the progressive breakage of bars, which naturally facilitates the representation of discontinuities, the interaction between multiple cracks, and the incorporation of stochastic material properties (Kosteski et al. (2012)). DEM has proven effective in addressing dynamic fracture, size effects, and unstable crack propagation, as well as in recent developments where it has been integrated with FEM formulations to extend its applicability to larger domains (Kosteski et al. (2024)).

On the other hand, the Phase Field Method (PFM) has emerged as a robust continuum-based alternative. This approach introduces a scalar damage field that describes the smooth transition between intact and fully fractured states, thereby eliminating the need for explicit crack tracking. Its variational foundation and ability to capture phenomena such as crack branching, coalescence, and deflection explain its increasing acceptance within the scientific community (Miehe et al. (2010); Duda et al. (2015); Tanné et al. (2018); Zambrano et al. (2022)). Moreover, PFM can be applied to a wide range of fracture regimes, from brittle to quasi-brittle materials, under both static and dynamic conditions.

Despite the significant progress achieved by both methodologies, direct comparative studies remain scarce. Open questions persist regarding their relative performance in terms of computational cost, numerical robustness, accuracy in crack path prediction, and ability to represent material heterogeneity. In this context, systematic analyses are highly desirable to clearly identify the strengths and limitations of each approach. The present work addresses this issue by providing a comparative study between a truss-based Discrete Element Method (DEM) and a Phase Field formulation implemented within the FEM framework. The comparison is carried out through three representative examples: (i) a Single Edge Notch Bending (SENB) test in epoxy resin, (ii) a Notched Plate with Hole (NPWH) test, and (iii) a parametric study of a specimen composed of a substrate, and an interface orthogonal to the crack propagation direction. The analysis of these cases allows for a detailed assessment of the response of both methods in different quasi-brittle fracture scenarios, establishing criteria for their applicability and providing insights for selecting the most suitable technique depending on the problem under study.

## 2 METHODOLOGY AND RESULTS

Reference problems in Fracture Mechanics, specifically within the context of quasi-brittle fracture, are solved by implementing both the truss-based Discrete Element Method (DEM) and the Phase Field Method (PFM) within the FEM framework. Regarding the DEM, in the formulation employed here, the continuum is spatially discretized into regular lattice modules, with the stiffness of the bars (elements) defined in such a way that their overall behavior is equivalent to that of the continuum being represented. The mass of the model is discretized and concentrated at the nodes. Fig. 1 shows a module composed of eight nodes located at the vertices plus a central node. Each node has three associated degrees of freedom, corresponding to the spatial components of the displacement field $\mathbf{u}$. The nodal masses are connected by longitudinal and diagonal elements of lengths $L_c$ and $\frac{\sqrt{3}}{2}L_c$, respectively. The equivalence between this cubic arrangement and an orthotropic elastic solid, with the material principal axes aligned along the longitudinal elements, was verified by Hayashi (1982) within the framework of linear elasticity. A restriction of $\nu = 0.25$ on Poisson's ratio must be imposed to achieve perfect equivalence. For other values of $\nu$, small differences appear in the shear terms; however, these discrepancies can be neglected, particularly when the focus is on the nonlinear response of the model under study.

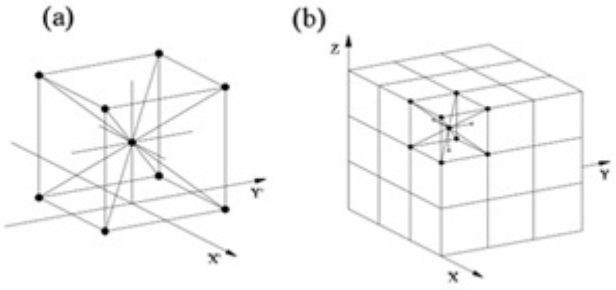


Figure 1: (a) Detail of the basic cubic module, (b) Prism composed of several cubic modules.

In the case of materials with a linear elastic constitutive law, the equation of motion of the system with N degrees of freedom, resulting from the spatial discretization, can be expressed as:

$$\mathbf{M}.\ddot{\mathbf{u}} + \mathbf{K}.\mathbf{u} = \mathbf{q}(t), \tag{1}$$

where $\mathbf{M}$ denotes the (diagonal) mass matrix, $\mathbf{u}$ and $\ddot{\mathbf{u}}$ represent the nodal displacement and acceleration vectors, respectively. The term $\mathbf{q}(t)$ is the vector containing the applied external forces. System $(1)$ can be numerically integrated in the time domain using a classical explicit integration scheme (the central difference finite difference method). On the other hand, Rocha (1989) proposed a bilinear constitutive relation for the elements, which allows modeling the brittle failure of the material. The general form is given by:

$$Force = function(bar\ deformation), \tag{2}$$

This constitutive relation is illustrated in Fig. 2, where $P_{cr}$ denotes the maximum tensile force transmitted by the element, and $\epsilon_p$ is the strain associated with $P_{cr}$. For $\epsilon < \epsilon_p$, the unloading process is linear up to the origin. However, when $\epsilon \geq \epsilon_p$, unloading occurs with a reduced slope, reflecting the stiffness degradation due to damage (Fig. 2b). The critical strain, $\epsilon_p$, is defined as:

$$\epsilon_p = \sqrt{\frac{G_f}{E.d_{eq}}}, \tag{3}$$

where $G_f$ is the average fracture energy associated with the length of the adopted DEM basic module, $L_c$. The parameter $d_{eq}$ is a material characteristic length, analogous to the plastic zone width at the crack tip in the Dugdale model. The area under the curve represents the energy density required to break the element, and it is defined using the relation between the fracture energy, $G_f$ (a material property), and the characteristics of the DEM model. $E_A$ is a constant proportional to the bar stiffness that relates the previous parameters ($P_{cr} = E_A.\epsilon_p$). Finally, $k_r$ is the parameter that determines the ultimate strain at which the element loses its capacity to transmit stress, leading to the rupture strain $\epsilon_r$. In this way, the DEM accounts for both the nucleation of damage and the failure of specific regions of the model, which translates into the deactivation of elements that have exhausted their strength. At this point, it becomes evident that the parameters of the constitutive relationship do not depend solely on the material but also on the model discretization. Thus, $P_{cr}$, $\epsilon_p$, $\epsilon_r$ and $G_f$ are material-specific properties, while $A_f$ and $L_c$ are model-specific properties, and the parameters $E_A$ and $k_r$ depend on both the model and the material. Finally, it is worth noting that the method allows for the consideration of material property randomness by varying these parameters from element to element according to a defined statistical law.

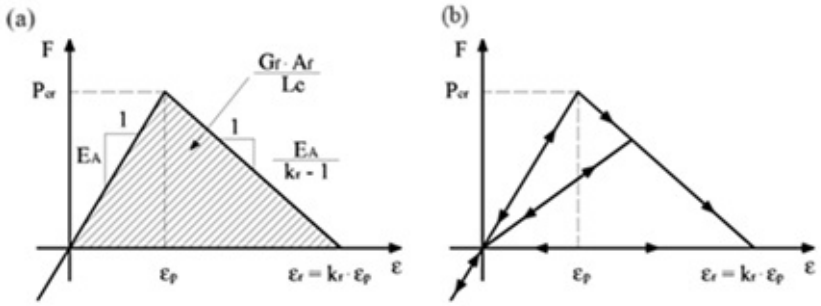


Figure 2: Elemental constitutive relationship of the truss bars. (a) Adopted constitutive diagram with its controlling parameters, (b) Schematic for loading and unloading.

On the other hand, in the context of the challenges associated with modeling discontinuous (discrete) cracks, this situation has motivated the development of other computational techniques in which crack paths are determined automatically as part of the solution. Among these numerical techniques, a currently very popular one is the Phase Field Model (PFM). This model is fundamentally based on the formulation for brittle fracture originally proposed by Francfort and Marigo (1998), which relies solely on Griffith's concept of the competition between the stored elastic energy of the body and the fracture energy. This fracture model is capable of addressing issues such as crack path and crack nucleation. In the original version by Francfort and Marigo, more in line with Linear Elastic Fracture Mechanics (LEFM), the concept of nucleation did not exist. In later versions, with a reinterpretation of the model parameters, the concept of nucleation can be addressed using this technique. As shown in Pham et al. (2011), Bourdin et al. (2014), and Nguyen et al. (2016), this method can potentially reconcile stress- and toughness-based criteria for crack nucleation, capture size effects relevant at both small and large length scales, and provide a robust and relatively simple approach for modeling crack propagation

in complex two- and three-dimensional environments. Therefore, consider a body B, which contains an arbitrary diffuse crack and is subjected to displacement and traction boundary conditions, as schematically illustrated in Fig. 3. The governing equations of the phase field model consist of a mechanical balance and a phase field balance, as presented below:

-Integral balance of mechanical forces:

$$\nabla \cdot \boldsymbol{\sigma} + \mathbf{b} = 0 \qquad \forall \mathbf{X} \in \beta, \tag{4}$$

$$\boldsymbol{\sigma} \cdot \mathbf{n} = \mathbf{t}^* \quad , \quad \forall \mathbf{X} \in \partial\beta_N^{\mathbf{u}}, \tag{5}$$

-Integral balance of the phase field:

$$\nabla \cdot \boldsymbol{\xi} - (\pi_a + \pi_r) = 0 \quad , \quad \forall \mathbf{X} \in \beta, \tag{6}$$

$$\boldsymbol{\xi} \cdot \mathbf{n} = \mathbf{0} \quad , \quad \forall \mathbf{X} \in \partial\beta_N^{\varphi}, \tag{7}$$

where $\boldsymbol{\sigma}$ is the Cauchy stress tensor, $\mathbf{b}$ is the vector of external forces per unit volume, and $\mathbf{n}$ is a normal vector to the surface of body $\beta$, where the displacement boundary conditions $\partial\beta_N^{\mathbf{u}}$ and traction $\mathbf{t}^*$ are also applied. On the other hand, $\boldsymbol{\xi}$ is the micro-stress parameter, and $\pi$ is the microforce parameter, which is divided into active and reactive components $(\pi_a + \pi_r)$, with the boundary condition in the phase field context being zero on the surface of body $\beta$.

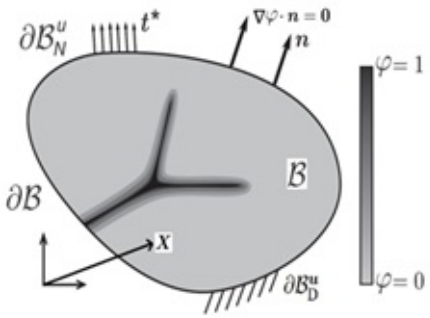


Figure 3: Body $\beta$ with an arbitrary diffuse crack and boundary $\partial\beta$

These equations are solved through a staggered solution procedure, which is a standard approach in variational fracture theory. Consequently, the phase field model has a scalar variable called the phase field $\varphi$, which varies within the interval $[0, 1]$. If $\varphi = 0$ at a point, it indicates that the material is unfractured. Conversely, if $\varphi = 1$ at a point, it is fully fractured. Values of $\varphi$ between zero and one correspond to partially fractured material. Points satisfying $\varphi = 1$ define cracks, i.e., traction-free surfaces embedded within the bulk material.

## 2.1 Application 1: Single Edge Notch Bending Tests (SENB)

The first reference problem addressed involves a SENB-type bar, whose dimensional scheme and boundary conditions are shown in Fig. 4a, with the following dimensional values: $W = 10.02x10^{-3}m,\ L = 46x10^{-3}m,\ B = 5.07x10^{-3}m,\ a_n = 4.9x10^{3}m,\ w_n = 0.35x10^{-3}m$. The material properties used were: Young's modulus $E = 3.51x10^{9}Pa$, Poisson's ratio $\nu = 2.5$, density $\rho = 1250\frac{Kg}{m^3}$, and fracture energy $G = 1010\frac{N}{m}$. The parameters implemented for the DEM simulations were: critical failure strain $\epsilon_p = 0.023\%$, cubic module length $L = 3x10^{-4}m$, time increment $\Delta t = 1.06x10^{-7}s$, and a characteristic material length $d_{eq} = 4.4x10^{-4}m$. The model discretization was performed using $153x34x16$

basic cubic modules, as shown in Fig. 1a, corresponding to a total of 1061351 bars. The configuration of the experimental test is shown in Fig. 4b, while the cracking patterns obtained with the Phase Field Model (PFM), using the same material properties as in the experiment with a characteristic length of $\ell_c = 0.06mm$, and with the DEM are illustrated in Figs. 4c and 4d.

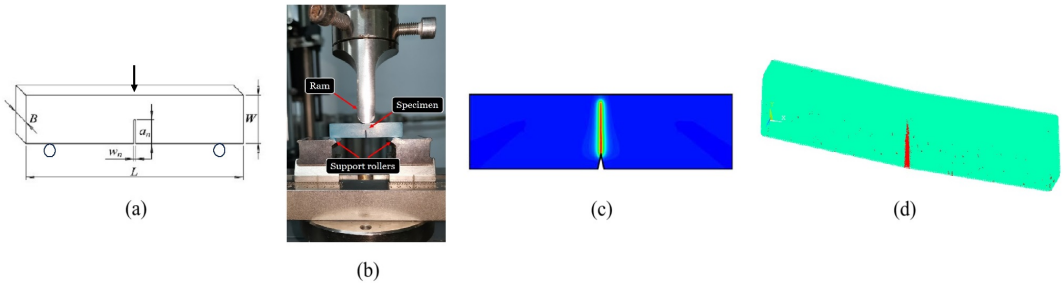


Figure 4: (a) Dimensional scheme and boundary conditions of the SENB model, b) Experimental test configuration, c) SENB bar results with the Phase Field model, d) Deformed SENB model with the DEM

As a result of the simulations carried out using the DEM and compared with both experimental results and numerical results obtained using a phase field model, taken from the work of Li et al. (2022), these results are graphically illustrated in Fig. 5.

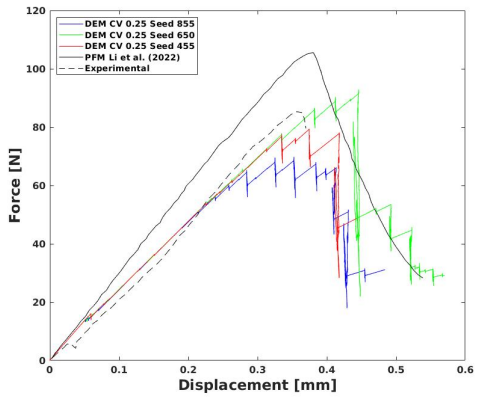


Figure 5: Comparative force-displacement plot for the SENB model

The plot in Fig. 5 shows the satisfactory performance of the simulations obtained with the DEM, which were conducted considering the randomness of material properties through a statistical law. In this particular case, a coefficient of variation (CV) of 0.25 was implemented, using three different seed values to generate the corresponding random distribution. These DEM results accurately capture the experimental behavior of the SENB model, even showing slightly better agreement than the curve obtained using the phase field method, which exhibits notable deviations from the experimental curve in both the elastic and post-critical stages. On a more general level, all problems modeled with the DEM achieved quite satisfactory convergence, although at a higher computational cost compared to the standard phase field model (Zambrano et al. (2024)). This cost can be reduced by implementing algorithmic optimization tools within the DEM computational framework. Furthermore, it is worth noting that the DEM, like the phase field model, has the advantage of not requiring a pre-defined crack in a given model to perform a simulation. Another advantage of the DEM is that its dynamic scheme allows for the consideration of randomness in material properties, which provides multiple benefits: it enables a more robust capture of various phenomena observed in experiments and allows for a more accurate interpretation of these results. In contrast, the phase field model presents a limitation in this regard.

## 2.2 Application 2: Notched Plate with Hole Tests (NPWH)

As a second benchmark problem, a compact tension test with a notch and a hole (NPWH) was addressed. The geometric representation, with dimensions expressed in "mm," together with the boundary conditions, is shown in Fig. 6a. The material properties adopted were: Young's modulus $E = 3.0x10^9 Pa$, Poisson's ratio $\nu = 2.5$, density $\rho = 1190\frac{Kg}{m^3}$, and fracture energy $G = 700\frac{N}{m}$. The parameters implemented in the DEM simulations were: critical failure strain $\epsilon_p = 0.023\%$, module length $L = 3x10^{-4}m$, time increment $\Delta t = 1.12x10^{-7}s$, and characteristic material length $d_{eq} = 8.82x10^{-4}m$. The simulations were performed under plane strain conditions. The discretization of the model was carried out with $500x400x2$ basic cubic modules, corresponding to a total of 2988312 bars. Accordingly, Fig. 6b shows the photoelasticity result of the experimental test, while Figs. 6c and 6d illustrate the configurations obtained with the Phase Field Model (PFM), taken from the work of Cavuoto et al. (2022), and the DEM technique, respectively. It can be observed that both numerical techniques (PFM and DEM) provide an excellent prediction of the crack trajectory for this problem, showing good agreement with the experimental crack propagation pattern.

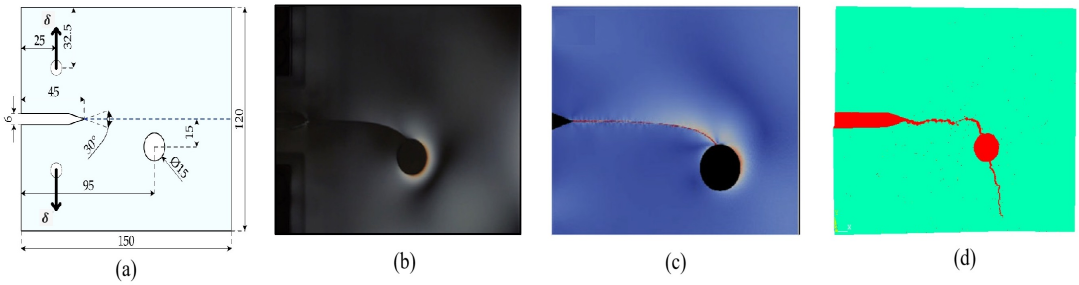


Figure 6: (a) Geometric scheme (measurements in "mm") and boundary conditions for the compact tension test, b) Experimental deformation for the NPWH, c) Deformation obtained with the Phase Field model for the NPWH, d) Deformation obtained with the DEM for the NPWH

The results of the simulations obtained with the DEM are presented in a force–displacement comparative plot in Fig. 7, where both the experimental curve from the compact tension test and the curve obtained with the Phase Field model are illustrated. The latter two curves were taken from the work of Cavuoto et al. (2022). Consequently, Fig. 7 shows the three curves obtained with the DEM using a coefficient of variation (CV) of 0.5 with three different seed values, reflecting the method's inherent randomness. The curves exhibit satisfactory behavior, although some differences with the experimental compact tension test curve are observed, both in terms of the maximum force reached and the amount of energy dissipated. The dissipated energy in the numerical curves is considerably higher than in the experiment, as the area under the curve is much larger. One possible approach to address this discrepancy would be a more thorough calibration of the DEM simulations. Regarding the curve obtained with the Phase Field model, it also shows some differences compared to both the experimental curve and the DEM numerical curves.

## 2.3 Application 3: Analysis of the interaction of a propagating crack with an interface

The third benchmark problem is a standard case in fracture mechanics, concerning the interaction of a propagating crack with an interface. A plate with an interface orthogonal to the crack propagation direction is modeled, with the following dimensions: $a = b = 0.01m$, as shown in Fig. 8a along with the corresponding boundary conditions. Plane strain conditions are considered. This plate is composed of two materials: a substrate material, which contains a pre-crack and serves as the medium through which the crack initiates propagation, and the interface material present in the specimen. The substrate properties implemented were: Young's modulus $E = 3.3x10^9 Pa$, Poisson's ratio $\nu = 2.5$, density $\rho = 1188\frac{Kg}{m^3}$, and fracture energy $G = 810\frac{N}{m}$. The initial properties of the interface were set equal to those

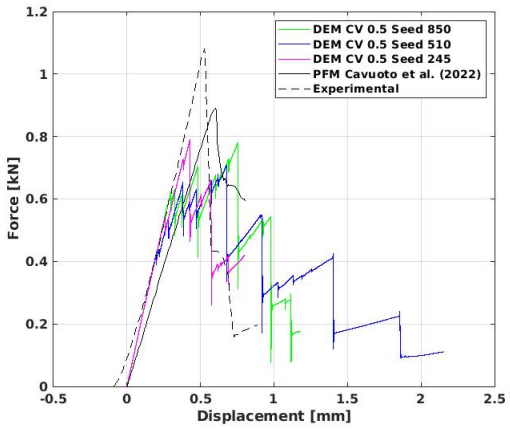


Figure 7: Comparative force–displacement plot for the NPWH tests

of the substrate and were varied using dimensionless ratios to obtain different factors for configuring the DEM simulations. These dimensionless ratios are as follows: (i) the ratio of the fracture energies of the substrate and the interface, (ii) the ratio of the critical strengths of the substrate and the interface, and (iii) the ratio of the $K_r$ coefficients, a parameter related to the material properties and the size of the basic cubic module. This coefficient ensures the stability of the DEM computational algorithm, which must satisfy $K_r > 1.1$. The discretization of the plate was carried out with $100x100x2$ basic cubic modules, as illustrated in Fig. 8b, corresponding to a total of $147412$ bars.

Regarding the results obtained for this third problem, they can be observed in Figs. 8c and 8d. The DEM simulations show a satisfactory capture of the penetration (Fig. 8c) and deflection (Fig. 8d) mechanisms of a crack interacting with an interface orthogonal to the crack propagation direction. The penetration mechanism corresponds to the case in which the crack propagates through medium 1, strikes the interface, and crosses it, continuing its propagation into medium 2. Conversely, the deflection mechanism occurs when the crack propagates through medium 1, strikes the interface, and deviates along the interface. It is also important to highlight the presence of a third mechanism, termed crack deviation out of the interface, in which the crack, once propagating through the interface, seeks to exit it and propagate into medium 2. This mechanism can be observed in Fig. 8d. Consequently, these results emphasize that the DEM is anumerical technique with excellent capability to represent material heterogeneity.

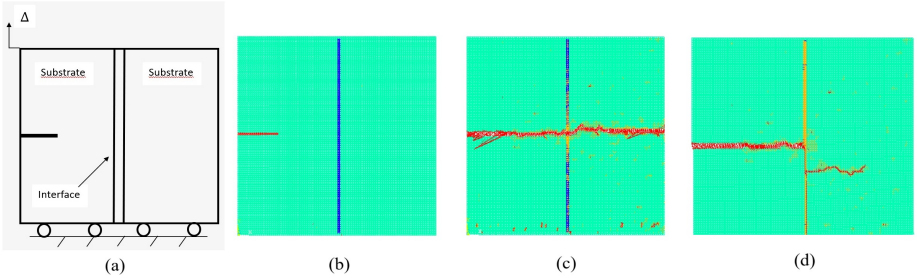


Figure 8: (a) Geometric scheme of the plate composed of a substrate and an interface, (b) DEM discretization of the plate under study, (c) Penetration mechanism of a crack interacting with an interface, (d) Deflection mechanism of a crack interacting with an interface

Finally, Figs. 9a and 9b show plots constructed in a dimensionless space, with the vertical axis representing the ratio of the fracture energies of the substrate and the interface, and the horizontal axis representing the ratio of the critical strengths of the substrate and the interface. The red points connected by a solid red line indicate the boundary where the deflection mechanism of a propagating crack interacting with an interface occurs, while the blue points connected by a solid blue line indicate the boundary

where the penetration mechanism occurs, i.e., a crack propagating through one medium crosses an interface. Each point in the plots corresponds to a simulation performed with both the DEM and the PFM, the latter taken from the work of Zambrano et al. (2022), and in both plots the presence of each mechanism (penetration and deflection) was verified. It is noteworthy that the overall behavior of both curves satisfactorily captures a mixed criterion of strength and toughness that characterizes the deflection and penetration mechanisms of a propagating crack interacting with an interface. Moreover, the behavior of the DEM-derived plot qualitatively agrees with the plot obtained using the PFM in the study by Zambrano et al. (2022). It is also important to note that the DEM curves do not extend above $\frac{G_s}{G_i} = 2$ on the vertical axis due to the limitations of the discretization used. Therefore, employing a finer discretization would allow further extension of these curves.

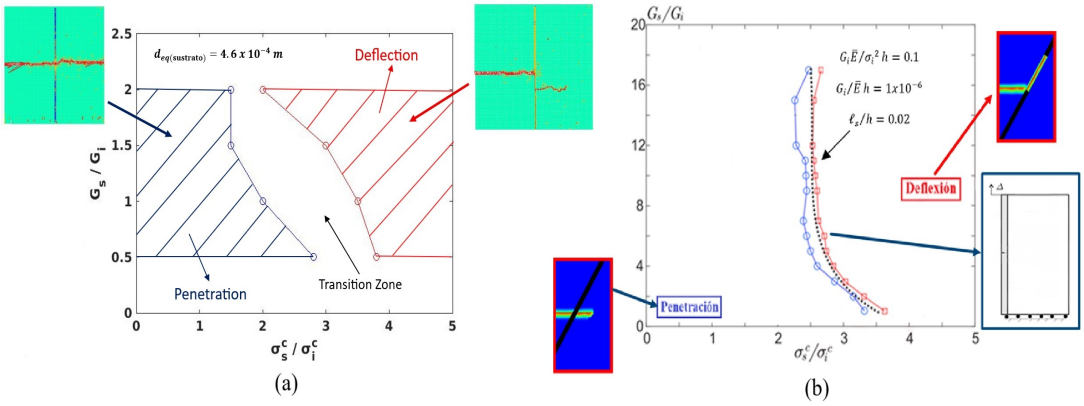


Figure 9: Graphical behavior of the penetration and deflection mechanisms of a propagating crack interacting with an interface orthogonal to its propagation direction: a) DEM modeling, b) Phase Field modeling taken from Zambrano et al. (2022)

## 3 CONCLUSIONS

The Discrete Element Method (DEM) based on truss-type bars is an alternative numerical technique that allows modeling quasi-brittle fracture problems. It essentially consists of the spatial discretization of the continuum using regular lattice modules, defined in such a way that their behavior is equivalent to that of the continuum being represented. Therefore, it emerges as a valuable numerical alternative, alongside others existing in the literature, particularly the phase field model (PFM), which represents an arbitrary crack in a body in a diffuse manner using a scalar variable called the phase field. Consequently, in the various benchmark problems modeled using the DEM, the technique demonstrates satisfactory performance in robustly capturing the physics of these problems, yielding results with very good accuracy and, in some cases, even surpassing the precision achieved by the phase field model. Furthermore, the DEM provides excellent prediction of crack trajectories, showing excellent agreement with experimental observations and a high capability for representing material heterogeneity. Additionally, the DEM has the advantage of incorporating randomness in material properties, which is not considered in the phase field model (PFM). The DEM achieves excellent convergence in each of the reference problems modeled, although it entails a higher computational cost compared to other numerical techniques, particularly the phase field model (PFM). This limitation could be mitigated by implementing algorithmic optimization tools within the DEM computational framework, which will be addressed in future work.

## REFERENCES

Bourdin B., Marigo J.J., Maurini C., and Sicsic P. Morphogenesis and propagation of complex cracks induced by thermal shocks. *Physical review letters*, 112:014–301, 2014. http://doi.org/10.1103/PhysRevLett.112.014301.

Cavuoto R., Lenarda P., Misseroni D., Paggi M., and Bigoni D. Failure through crack propagation in components with holes and notches: An experimental assessment of the phase field model. *International Journal of Solids and Structures*, 257:111–798, 2022. http://doi.org/10.1016/j.ijsolstr.2022.111798.

Duda F.P., Ciarbonetti A., Sánchez P.J., and Huespe A.E. A phase-field/gradient damage model for brittle fracture in elastic–plastic solids. *International Journal of Plasticity*, 65:269–296, 2015. http://doi.org/10.1016/j.ijplas.2014.09.005.

Francfort G. and Marigo J.J. Revisiting brittle fracture as an energy minimization problem. *Journal of the Mechanics and Physics of Solids*, 46:1319–1342, 1998. http://doi.org/10.1016/S0022-5096(98)00034-9.

Hayashi Y. *Sobre um modelo de discretização de estruturas tridimensionais aplicado em dinâmica não linear*. Ph.D. thesis, Universidade Federal do Rio Grande do Sul, Porto Alegre, Brasil, 1982. http://doi.org/INIS-BR–135.

Kosteski L., Barrios D'Ambra R., and Iturrioz I. Crack propagation in elastic solids using the truss-like discrete element method. *International journal of fracture*, 174:139–161, 2012. http://doi.org/10.1007/s10704-012-9684-4.

Kosteski L., Iturrioz I., Galiano Batista R., and Cisilino A.P. The truss-like discrete element method in fracture and damage mechanics. *Engineering Computations*, 28:765–787, 2011. http://doi.org/10.1108/02644401111154664.

Kosteski L.E., Friedrich L.F., Costa M.M., Bremm C., Iturrioz I., Xu J., and Lacidogna G. Fractal scale effect in quasi-brittle materials using a version of the discrete element method. *Fractal and Fractional*, 8:678, 2024. http://doi.org/10.3390/fractalfract8120678.

Li Y., Huang K., Yu H., Hao L., and Guo L. Experimentally validated phase-field fracture modeling of epoxy resins. *Composite Structures*, 279:114–806, 2022. http://doi.org/10.1016/j.compstruct.2021.114806.

Miehe C., Hofacker M., and Welschinger F. A phase field model for rate-independent crack propagation: Robust algorithmic implementation based on operator splits. *Computer Methods in Applied Mechanics and Engineering*, 199:2765–2778, 2010. http://doi.org/10.1016/j.cma.2010.04.011.

Nguyen T.T., Yvonnet J., Bornert M., Chateau C., Sab K., Romani R., and Roy R.L. On the choice of parameters in the phase field method for simulating crack initiation with experimental validation. *International Journal of Fracture*, 197:213–226, 2016. http://doi.org/10.1007/s10704-016-0082-1.

Pham K., Amor H., Marigo J.J., and Maurini C. Gradient damage models and their use to approximate brittle fracture. *International Journal of Damage Mechanics*, 20:618–652, 2011. http://doi.org/10.1177/1056789510386852.

Rocha M.M. *Ruptura e efeito de escala em materiais não-homogêneos de comportamento frágil*. Ph.D. thesis, Universidade Federal do Rio Grande do Sul, Porto Alegre, Brasil, 1989. http://doi.org/hdl.handle.net/10183/170724.

Tanné E., Li T., Bourdin B., Marigo J.J., and Maurini C. Crack nucleation in variational phase-field models of brittle fracture. *Journal of the Mechanics and Physics of Solids*, 110:80–99, 2018. http://doi.org/10.1016/j.jmps.2017.09.006.

Zambrano J., Toro S., Sánchez P.J., Duda F.P., Méndez C.G., and Huespe A.E. Interaction analysis between a propagating crack and an interface: Phase field and cohesive surface models. *International Journal of Plasticity*, 156:103–341, 2022. http://doi.org/10.1016/j.ijplas.2022.103341.

Zambrano J., Toro S., Sánchez P.J., Duda F.P., Méndez C.G., and Huespe A.E. An arc-length control technique for solving quasi-static fracture problems with phase field models and a staggered scheme. *Computational Mechanics*, 73:751–772, 2024. http://doi.org/10.1007/s00466-023-02388-7.